Muscle Architecture Parameters Inferred from Simulated Single-Element Ultrasound Traces

Letizia Gionfrida[1,2†], Daekyum Kim[3†], Yichu Jin[2†], Conor J. Walsh[2], Robert D. Howe[2]

***Abstract*— Wearable robots have shown great promise in aiding individuals with reduced mobility and enhancing human performance across various applications. To achieve optimal assistance, accurate estimation of muscle dynamics has shown promise in designing adaptive control strategies. Among different techniques, B-mode ultrasonography produced with linear array transducers have gained popularity as a gold-standard imaging tool, providing non-invasive solutions to measure in-vivo muscle dynamics. B-mode ultrasound has been employed to infer muscle thickness, fascicle lengths, pennation angles, and muscle force using neural networks, offering a valuable tool for designing individualized control strategies. The effectiveness of this measuring tool depends on integrating transducers into the wearable robot, but B-mode relies on large transducers. Studies have explored smaller single-element transducers for better wearability for muscle thickness estimation. However, their ability to infer more complex muscle architecture parameters using automated techniques is yet to be determined. In this study, we propose an approach to extract M-mode traces from B-mode images to simulate signals from single-element transducers. We then employ various machine learning architectures to infer muscle pennation angle and fascicle length. Preliminary results indicate promising performance from the CNN+Transformer (2-layer spatial) + Transformer (2-layer temporal) models, with results from the CNN+LSTM models (with a RMSE of 0.02 radian for pennation angle and 2.54mm for fascicle lengths). This study paves the way for enabling the use of smaller and more portable single-element transducers for wearable robotic applications. The link to the code is https: https://github.com/raku-slyu/AB-Mode-Utrasound.**

I. Introduction

Wearable robots have shown great potential in assisting individuals with reduced mobility and enhancing human performance [1][2]. Inspired by the direct coupling between muscle force and changes in muscle architecture parameters [3], [4], such as muscle thickness, fascicle length, and pennation angle, sensing these parameters has played an important role for realizing individualized control strategies for wearable robots [5], [6], [7], [8]. Ultrasound is a non-invasive imaging tool that has been commonly used to measure muscle structure and dynamics.

Brightness mode (B-mode) ultrasound has been widely used for estimating muscle thickness [9], fascicle lengths [10], [11], pennation angles [12], and muscle force [13], [14]. B-mode ultrasound uses linear array transducers to form 2D images of the underlying muscles. Despite the rich information contained in these images, B-mode ultrasound often relies on bulky transducers (Fig. 1), sophisticated instruments, and computationally intensive algorithms for image formation and processing. The integration of these larger linear array transducers into wearable robotic systems can pose challenges and increase costs [15]. Alternatively, motion mode (M-mode) ultrasound obtained using single-element transducers (SETs) offers a potential lightweight solution for muscle dynamics measurement. Such ultrasound modality uses the smaller SETs (e.g., 1 x 1 x 1 cm^3, Fig 1) to record 1D scans of the muscle over time. Without relying on 2D images, M-mode ultrasound can be produced without using complex image processing algorithms and associated instrumentation.

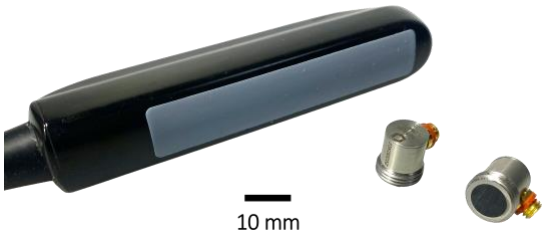

Fig. 1. Illustration of an example linear array transducer (LV8-4L65S-3, Telemed) and two single-element transducers (Alpha 113-124-660, Waygate Technologies).

Previous research has developed algorithms for estimation of muscle architecture parameters using B-mode ultrasound imaging [10], [11], [16], [17], [18]. However, to the best of our knowledge, deriving muscle architecture parameters with data from SETs has been rarely studied. Specifically, although there has been a prior attempt to gauge muscle thickness with one-dimensional ultrasound [19], obtaining changes in muscle fascicle length and pennation angle remain challenging with SETs. Due to the direct link among fascicle length, pennation angle, and muscle force [20], [21], such an investigation has the potential to enhance the adoption of SET-based ultrasound for developing effective and adaptive control strategies for wearable assistive robots.

In this study, our objective is to investigate the inference of muscle fascicle lengths and pennation angles using SETs, bypassing the requirement for larger linear array transducers that produce B-mode images. The primary scope of this investigation is to ascertain whether the incorporation of images (B-mode) is indispensable for the accurate prediction of fascicle length and pennation angle, or if a smaller scan can suffice. To do so, we extracted M-mode traces from previously collected B-mode sequences [4], to simulate data as they would be collected from SETs. We then applied learning-based algorithms to evaluate the feasibility of inferring fascicle lengths and pennation angles from the simulated SET ultrasound traces (Fig. 2). This research could pave the way for integrating more compact ultrasound probes into wearable robotic systems, thereby improving the portability and usability of future wearable assistive robots.

[1] Department of Informatics, Faculty of Natural Mathematical and Engineering Sciences, King's College London, Bush House, London, WC2R 2LS, United Kingdom (email: letizia.gionfrida@kcl.ac.uk).
[2] John A. Paulson School of Engineering and Applied Sciences, Harvard University, Cambridge, MA, USA (email: {gionfrida, yichu_jin, walsh, howe}@seas.harvard.edu).
[3] School of Mechanical Engineering and the School of Smart Mobility, Korea University, Seoul 02841, South Korea (email: daekyum@korea.ac.kr).
[†] L. Gionfrida, D. Kim, Y. Jin contributed equally to this work.

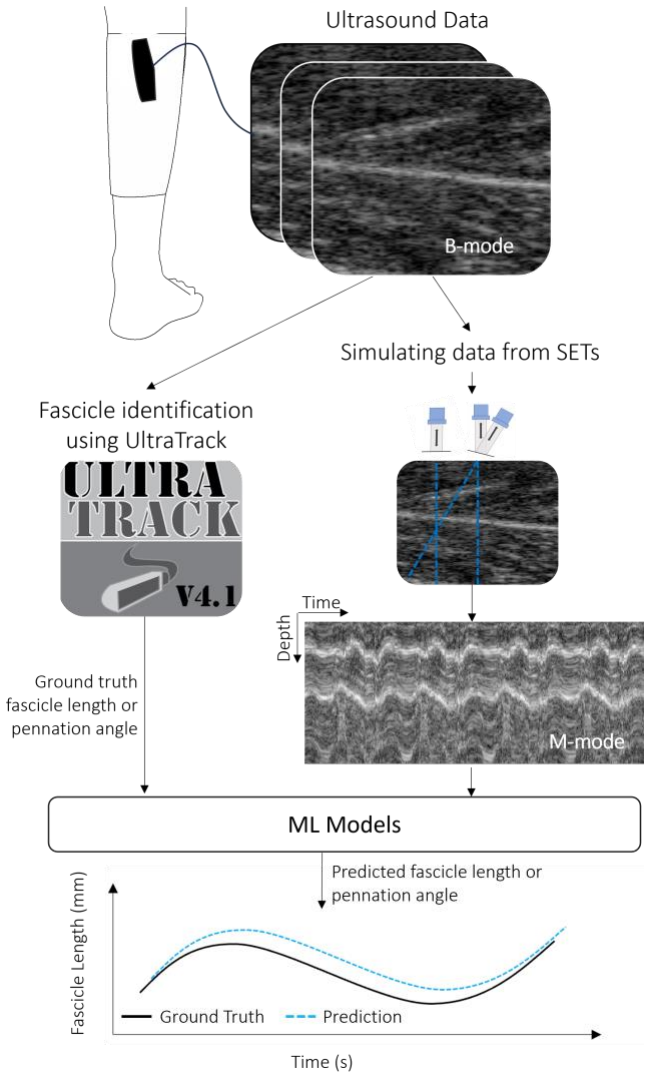

Fig. 2. The proposed study where from the collected B-mode ultrasound images, we extract pseudo-M-mode traces to simulate signals collected from single-element transducers. We then employ various machine learning techniques to infer changes in muscle pennation angle and fascicle length.

II. Methods

A. Participants

The data used in this study were previously collected in [7]. Nine participants (3 females and 6 males; age 29.1 ± 4.04 years (mean ± std)) participated in this study. None of the participants had a prior medical history of physical or neurological impairments or disabilities related to walking. The study was conducted in accordance with the Harvard Longwood Campus Institute Review Board, IRB-22086. The participants consented to the study protocol prior to the study.

B. Experiment procedure and study design

Each participant walked on a treadmill with the following conditions: level ground walking at speeds of 1.0m/s, 1.25m/s, 1.5m/s, and 1.75m/s, and walking at 5.71 degrees incline (10% incline) at 1.25m/s. The heel-strike events were detected using an instrumented treadmill (Bertec, Columbus, OH, USA; 1200HZ). Participants had a low-profile ultrasound transducer (MicroUs, Telemed, Vilnius, Lithuania) affixed to their left leg to monitor the medial gastrocnemius and soleus muscles. The ultrasound transducer collected images at a rate of 113Hz with a resolution of 512 x 512 pixels (width and height). A 75mm-wide ultrasound probe with a 5MHz center frequency was placed over the medial gastrocnemius, proximal to the gastrocnemius muscle-tendon junction. The probe was manually adjusted to ensure that the fascicles were in straight lines as much as possible. The probe was secured to the participant's limb using self-adhesive athletic tape (Coban) throughout the experiment.

C. Data pre-processing

The dataset consisted of 64,849 B-mode ultrasound image frames in total (equal to approximately 10 minutes recording) To obtain ground truth fascicle lengths and pennation angles, we labeled individual fascicle by selecting pixels belonging to muscle fascicles using UltraTrack [22]. Specifically, we used a combination of manual and semi-automated labeling techniques to minimize spatial drift caused by the affine optical flow introduced by UltraTrack over longer sequences, as in [10], to obtain fascicle lengths and pennation angles, partitioned based on pre-recorded heel strikes.

From the labelled B-mode ultrasound images, we extracted M-mode signals from nine different locations, as shown in Fig. 3. Specifically, we extracted pixel values along a straight line in each B-mode frame and then temporally concatenated these lines across all time frames. The line locations were selected to represent a diverse range of possible SET placements, with the anticipation that additional analysis would be conducted to identify the minimal required traces.

We employed the nine distinct sets of extracted M-mode traces (Fig 3.) as inputs to different computational models to estimate either fascicle length or pennation angle. In the M-mode traces, as the lengths of straight and angled lines differed, we applied zero padding at the end of angled line data to ensure uniformity in length across the simulated M-mode traces.

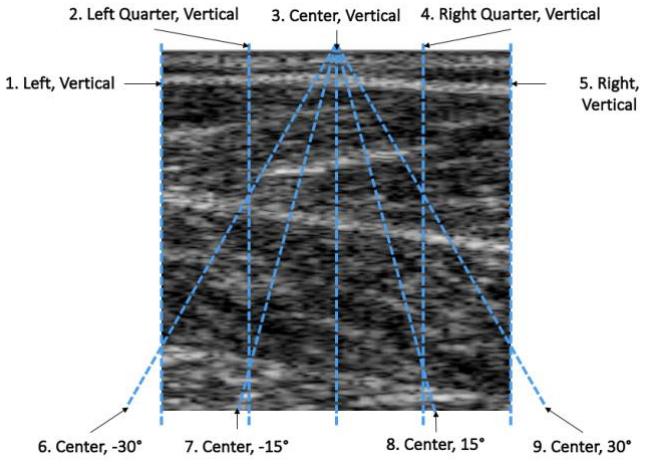

Fig. 3. Nine lines selected from B-mode images to generate simulated M-mode traces.

The simulated data served as input to the machine learning model which applied a time window ranging $t \triangleq 1, 2, \ldots, w$, where w is a window size that we vary from 3, 5, …, 11. Subsequently, we sampled the subsequent input and output data from $t=s$ to $t=s+w$, where s denotes a sliding stride length that we define is always $w+1$, not to make any overlap between data windows. This sampling process iterated based on the s and w parameters. The sliding window approach is a common approach to preprocess time series data to feed into a deep learning model [23], [24]. It also has been used in tasks in using ultrasound [25]. A detailed schematic is depicted in Fig. 4.

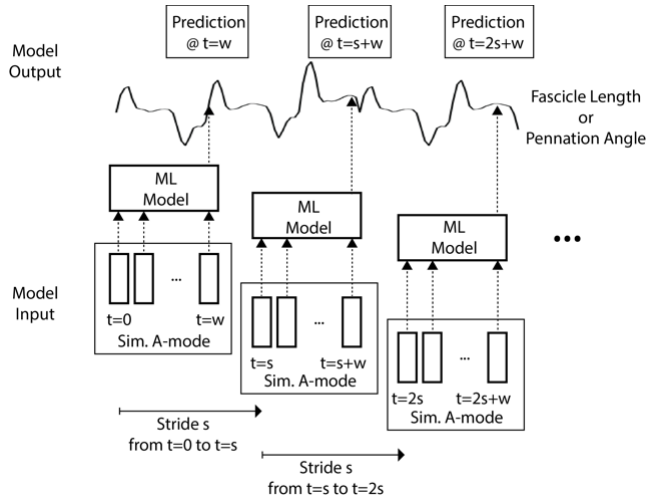

Fig. 4. Schematic of the model training procedure. Input data were extracted M-mode data with window length w and sliding stride length s. A machine learning model estimates either fascicle length or pennation angle of the previous time frame of the input time window.

Ultimately, for each trial, data from all participants and all conditions were randomly divided into training, validation, and test sets following a ratio of 60:15:25. The sequential arrangement of train/validation/test datasets in each trial was determined randomly. For example, in instances where the order is validation/train/test, the initial 15% of a trial was allocated as the validation dataset, the subsequent 60% was designated as the training set, and the final 25% was assigned to the test set. The order was determined through a random number generator.

D. Model architectures

In this study, five different frequently employed deep learning models were tested. The model architectures are illustrated in Fig. 5.

These models encompassed a 4-layer Long Short-Term Memory (LSTM) [26], a Convolutional Neural Network (CNN) [27] with an LSTM (CNN+LSTM) configuration with 4 layers [28], a hybrid model featuring 2 Spatial (S) layers and 2 Temporal (T) LSTM layers, a 4-layer CNN+Transformer (TR) [29], and a variant integrating 2 Spatial Transformer (ST) layers with 2 Temporal Transformer (TR) layers. LSTM, CNN, and Transformers have been used widely to process 1-dimensional temporal data across tasks. We tried CNN_ST_LSTM and CNN_ST_TR because ultrasound data have both spatial and temporal relationships. The first model runs across the spatial dimension, and the second model runs across the temporal dimension.

- **LSTM:** This model consisted of four LSTM layers stacked sequentially. Each LSTM layer took the hidden states from the previous layer as inputs and processed them to capture temporal dependencies in the data. We used 128 hidden features for each LSTM layer. The output of the final LSTM layer was the regression inference.
- **CNN_LSTM** (4-layer LSTM): The CNN+LSTM model with 4 layers combined a CNN and LSTM architecture. The ResNet18 CNN model without the final fully connected layer [30] was employed to extract spatial features from the input data. The output of the CNN component was then passed through four LSTM layers, which captured temporal dependencies in the sequence of spatial features. We used 128 hidden features for LSTM models. Finally, a fully connected layer was utilized for regression based on the LSTM output.
- **CNN_ST_LSTM**: This model incorporated both spatial and temporal neural network layers. The ResNet18 CNN without the final fully connected layer was employed to extract spatial features from the input data. The output of the CNN was then passed through two LSTM layers that focused on capturing spatial dependencies. The resulting spatial-temporal features were then fed into two additional LSTM layers that captured temporal dependencies across the sequence. We used 128 hidden features for LSTM models. Finally, a fully connected layer was utilized for classification.
- **CNN_TR**: The CNN+Transformer model with 4 layers combined a CNN and Transformer architecture. The ResNet18 CNN without the final fully connected layer was employed to extract spatial features from the input data. The output of the CNN component was then passed through four Transformer layers, which captured long-range dependencies and interactions between the spatial features. A fully connected layer was used for regression based on the Transformer output. We used number of heads to be the same as the window size for Transformer.
- **CNN_ST_TR**: This model extended the previous model by incorporating both spatial and temporal Transformer layers. The ResNet18 CNN without the final fully connected layer was employed to extract spatial features from the input data. The output of the CNN was then passed through two spatial Transformer layers, which captured interactions between the spatial features. The resulting spatial-temporal features were then fed into two temporal Transformer layers that captured dependencies across the sequence. Finally, a fully connected layer was used for classification based on the Transformer output.

The number of head in the spatial dimension was 8, and the number of head in the temporal dimension was set to be the same as the window size for Transformer.

We trained each model with *(w, s) = {(3, 4), (5,6), (7,8), (9,10)}* to evaluate the effect of window lengths. Each model minimized the loss between ground truth and predicted fascicle length or pennation angle using Mean Squared Error Loss. We used the Adam optimizer with learning rate of 0.001. We used *PyTorch* version 2.0.0.

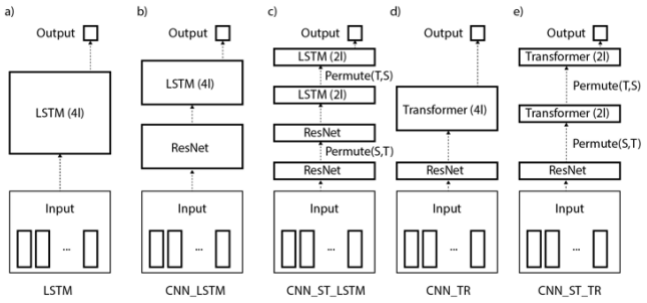

Fig. 5. Machine learning architectures used for model comparison including: a) a 4-layer (4l) Long Short-Term Memory (LSTM), b) a ResNet18 [30] Convolutional Neural Network (CNN) with an LSTM configuration with 4 layers, c) a two Spatial (S) LSTM layers (2l) and two Temporal (T) LSTM layers (2l) with a ResNet18 CNN, d) a ResNet18 CNN with a 4l Transformer (TR), and e) a 2 Spatial Transformer (ST) layer with 2 Temporal Transformer (TR) layer with a ResNet18 CNN.

III. RESULTS

A. Model Performance

Table I tabulates Root Mean Squared Error (RMSE) and Normalized Root Mean Squared Error (NRMSE) for each model that outputs the best performance. For both pennation angles and fascicle lengths, only models with the combinations of CNN and LSTM (indicated as CNN_LSTM and CNN_ST_LSTM) converged, suggesting they reached a point of stable and minimized errors. In contrast, other models including LSTM, CNN-Transformer (CNN_TR), and CNN-spatiotemporal Transformer (CNN_ST_TR) did not converge.

Among CNN-LSTM-based models, CNN-Spatiotemporal LSTM demonstrated the best performance, with the RMSE of 0.02 radian for pennation angle and 2.54 mm for fascicle lengths. These correspond to 1.6% and 2.3% NRMSE, respectively.

For estimating pennation angle, CNN-spatiotemporal LSTM produced the best performance when the window size=11, which corresponds to around 0.1 seconds. For fascicle length, the best performance occurred when the window size was 5, which is around 0.05 seconds. Figure 6 illustrates exemplar predicted pennation angles and fascicle lengths for 10 seconds.

TABLE I. RMSE AND NRMSE FOR EACH MODELACROSS PARTICIPANTS AND TASKS

	Model	Window length	Stride	RMSE (rad)	NRMSE (%)
Pennation angles	LSTM*	7	8	0.248	18.29
	CNN_LSTM	11	12	0.029	2.16
	CNN_ST_LSTM	11	12	**0.021**	**1.57**
	CNN_TR	11	12	0.070	5.16
	CNN_ST_TR	9	10	0.099	7.37
	Model	**Window length**	**Stride**	**RMSE (mm)**	**NRMSE (%)**
Fascicle lengths	LSTM*	3	4	17.952	16.01
	CNN_LSTM	11	12	2.559	2.45
	CNN_ST_LSTM	5	6	**2.543**	**2.29**
	CNN_TR*	11	12	19.700	18.85
	CNN_ST_TR*	11	12	18.178	17.39

*models not converged

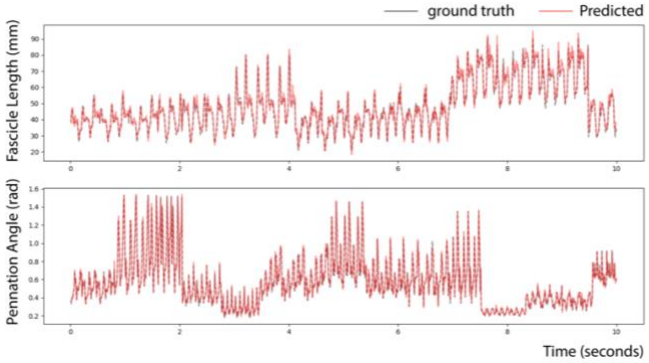

Fig. 6. An example plots of estimated pennation angle, in radian (rad), and fascicle length, in millimeters (mm), for the CNN_ST_LSTM model with the best window lengths and strides (i.e., *w*=11, *s*=12 for pennation angle, and *w*=5, *s*=6 for fascicle length).

B. Parameter study

We further conducted a parameter study to evaluate the impact of varying window size on each machine learning model.

The CNN_ST_LSTM consistently exhibited superior performance in estimating both fascicle length and pennation angle. Particularly, CNN_LSTM and CNN_ST_LSTM estimated fascicle length within 10 mm in RMSE, while other models produced less accurate results, with RMSE values reaching around 20 mm across different window lengths. On the other hand, for CNN_LSTM and CNN_ST_LSTM, the results were similar regardless of the window sizes.

For pennation angle, all the models, except LSTM, had errors around 0.1 radian. LSTM did not work well regardless of the window sizes. The parametric study is illustrated in Fig. 7.

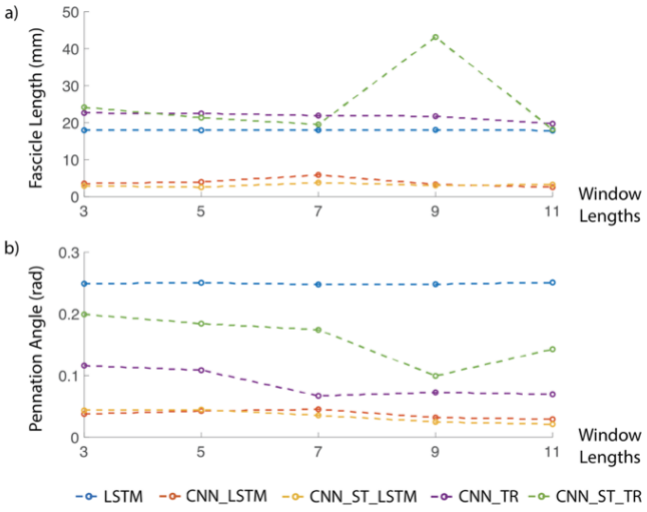

Fig. 7. Parameter study showing the effect on window length *w* for a) fascicle lengths in in millimeters (mm), and b) estimated pennation angle, in radian (rad) for the Long Short-Term Memory (LSTM), the Convolutional Neural Network (CNN) with an LSTM, the Spatial (S) and Temporal (T) CNN-LSTM, the CNN with a Transformer (TR), and a CNN with Spatial Transformer (ST) and Temporal Transformer (TR) layers.

IV. Discussion

In this study, we evaluated the feasibility of different machine learning algorithms to estimate changes in muscle fascicle length and pennation angle during walking using M-mode ultrasound data extracted from B-mode sequences. We conducted sensitivity analysis on model type, window length, and stride length to understand the performance of different algorithm configurations. Our work would provide valuable insights that can steer the development of future SET-based wearable ultrasound systems that can be seamlessly integrated into wearable robotic systems for enhanced control [31].

Our results are particularly notable due to the achievement of comparable accuracy with significantly less data compared to existing literature. In particular, our algorithm achieved fascicle length and pennation angle estimation with errors less than 2.6 mm and 1.3 deg, respectively. Prior studies on estimating gastrocnemius fascicle length have reported errors ranging from 2.36 to 4.7 mm using support vector machine [16] and deep neural network [10]. Similarly, prior studies on pennation angle estimation reported errors ranging from 0.43 to 1 deg using gradient boosting [32], clustering method [12], and deep residual networks [18]. However, these prior methods rely on full B-mode ultrasound images, requiring the use of linear array transducers. Our proposed method produced comparable estimation results with only M-mode ultrasound data, which could practically be obtained using SETs.

In our pursuit of superior predictive models, we conducted a sensitivity analysis on the effect of deep learning architecture. It is evident that the CNN-spatiotemporal LSTM model emerged as the most robust performer. The selection of this model can be attributed to its ability to harness spatial and temporal information effectively. Furthermore, our sensitivity analysis on window length and stride length provided critical insights into the optimal parameter configurations, emphasizing the importance of parameter tuning in predictive modeling. A well-optimized window length allows the model to encapsulate the appropriate contextual information from the input sequence, providing a balanced perspective for analysis. Meanwhile, the selected stride length contributes to how frequently the model processes these windows, influencing the granularity and overlap of information considered by the model.

Although the B-mode data were gathered during dynamic walking tasks, this study did not specifically assess the inference performance concerning variations in fascicle length and pennation angle across different walking speeds and incline levels. Previous studies utilizing B-mode imaging for inferring muscle architecture parameters have not conclusively linked the inference performance of fascicle length and pennation to specific variations in walking tasks. To fortify and draw more conclusive connections, future investigations will focus on evaluating these relationships, enhancing our understanding of how changes in walking dynamics correspond to alterations in fascicle length and pennation angle for single element traces.

It is worth noting that our extracted M-mode data may not fully represent those collected using SETs. The simulated data in our study exhibited a width equivalent to one pixel, a distinction from real M-mode that often manifests as several millimeters wide near the point of origin and may extend to a centimeter or more at greater depths. Further exploration could study the impact of varying widths on simulated M-mode samples on estimation accuracies of fascicle length and pennation angle. Furthermore, B-mode images, which serve as the foundation for our extracted M-mode signals, undergo an intricate signal processing pipeline. Such pipeline involves high-rate sampling of acoustic signals, beam forming, envelope detection, and final interpolation for 2-D display. In our study, this B-mode image formation sequence is succeeded by the sampling of images to create pseudo-M-mode signals. While these processing steps introduce variances from signals generated by SETs, it is essential to recognize that the fundamental acoustic transduction process, primarily reflection from variations in tissue acoustic impedance, remains consistent for both B-mode imaging and signals collected with SETs. Despite the defined disparities, the promising outcomes of our study prompt a call for further investigations using real-world SETs.

While this study represents a step towards realizing wearable ultrasound systems for muscle architecture parameter estimation, certain limitations and avenues for future research remain. To enhance practicality and broad applicability, further research is needed to develop generalized models that are adaptable to a diverse range of individuals. Additionally, it is important to acknowledge that the extracted M-mode ultrasound data used in this study may not perfectly mirror real signals obtained using SETs. Future work should investigate estimating changes in muscle architecture parameters with real traces collected using SETs.

V. Conclusion

In conclusion, our study provides evidence of the potential of wearable ultrasound systems in the context of wearable robotic systems. The achieved accuracy and robust model performance underline the feasibility of fast muscle parameter estimation, propelling us closer to the realization of integrated wearable ultrasound systems for enhanced control and user support. With ongoing research and refinement, the integration of this technology could pave the way for safer and more efficient wearable robotics, benefiting a wide range of applications from healthcare to industrial assistance.

References

[1] Siviy, Christopher, Lauren M. Baker, Brendan T. Quinlivan, Franchino Porciuncula, Krithika Swaminathan, Louis N. Awad, and Conor J. Walsh. "Opportunities and challenges in the development of exoskeletons for locomotor assistance." Nature Biomedical Engineering 7, no. 4 (2023): 456-472.

[2] Zhou, Yu Meng, Cameron J. Hohimer, Harrison T. Young, Connor M. McCann, David Pont-Esteban, Umut S. Civici, Yichu Jin et al. "A portable inflatable soft wearable robot to assist the shoulder during industrial work." Science Robotics 9, no. 91 (2024): eadi2377.

[3] Alvarez, Jonathan T., Ariane de Marcillac, Yichu Jin, Lucas F. Gerez, Oluwaseun A. Araromi, and Conor J. Walsh. "Surface-Level Muscle Deformation as a Correlate for Joint Torque." Advanced Materials Technologies: 2400444.

[4] Roberts, Thomas J., Carolyn M. Eng, David A. Sleboda, Natalie C. Holt, Elizabeth L. Brainerd, Kristin K. Stover, Richard L. Marsh, and Emanuel Azizi. "The multi-scale, three-dimensional nature of skeletal muscle contraction." Physiology 34, no. 6 (2019): 402-408.

[5] Xue, Xiangming, Bohua Zhang, Sunho Moon, Guo-Xuan Xu, Chih-Chung Huang, Nitin Sharma, and Xiaoning Jiang. "Development of a wearable ultrasound transducer for sensing muscle activities in assistive robotics applications." Biosensors 13, no. 1 (2023): 134.

[6] Yin, Zongtian, Hanwei Chen, Xingchen Yang, Yifan Liu, Ning Zhang, Jianjun Meng, and Honghai Liu. "A wearable ultrasound interface for prosthetic hand control." IEEE journal of biomedical and health informatics 26, no. 11 (2022): 5384-5393.

[7] Nuckols, Richard W., Sangjun Lee, Krithika Swaminathan, Dorothy Orzel, Robert D. Howe, and Conor J. Walsh. "Individualization of exosuit assistance based on measured muscle dynamics during versatile walking." Science robotics 6, no. 60 (2021): eabj1362.

[8] Nuckols, Richard W., Taylor JM Dick, Owen N. Beck, and Gregory S. Sawicki. "Ultrasound imaging links soleus muscle neuromechanics and energetics during human walking with elastic ankle exoskeletons." Scientific reports 10, no. 1 (2020): 3604.

[9] Cronin, Neil J., Taija Finni, and Olivier Seynnes. "Fully automated analysis of muscle architecture from B-mode ultrasound images with deep learning." arXiv preprint arXiv:2009.04790 (2020).

[10] Gionfrida, Letizia, Richard W. Nuckols, Conor J. Walsh, and Robert D. Howe. "Age-Related Reliability of B-Mode Analysis for Tailored Exosuit Assistance." Sensors 23, no. 3 (2023): 1670.

[11] Gionfrida, Letizia, Richard W. Nuckols, Conor J. Walsh, and Robert D. Howe. "Improved fascicle length estimates from ultrasound using a U-net-LSTM framework." In 2023 International Conference on Rehabilitation Robotics (ICORR), pp. 1-6. IEEE, 2023.

[12] Bao, Xuefeng, Qiang Zhang, Natalie Fragnito, Jian Wang, and Nitin Sharma. "A clustering-based method for estimating pennation angle from B-mode ultrasound images." Wearable Technologies 4 (2023): e6.

[13] Bohm, Sebastian, Falk Mersmann, Alessandro Santuz, and Adamantios Arampatzis. "The force–length–velocity potential of the human soleus muscle is related to the energetic cost of running." Proceedings of the Royal Society B 286, no. 1917 (2019): 20192560.

[14] Sartori, Massimo, and Gregory S. Sawicki. "Closing the loop between wearable technology and human biology: a new paradigm for steering neuromuscular form and function." Progress in Biomedical Engineering 3, no. 2 (2021): 023001.

[15] Xue, Xiangming, Bohua Zhang, Sunho Moon, Guo-Xuan Xu, Chih-Chung Huang, Nitin Sharma, and Xiaoning Jiang. "Development of a wearable ultrasound transducer for sensing muscle activities in assistive robotics applications." Biosensors 13, no. 1 (2023): 134.

[16] Rosa, Luis G., Jonathan S. Zia, Omer T. Inan, and Gregory S. Sawicki. "Machine learning to extract muscle fascicle length changes from dynamic ultrasound images in real-time." PloS one 16, no. 5 (2021): e0246611.

[17] Ashkani Chenarlogh, Vahid, Mostafa Ghelich Oghli, Ali Shabanzadeh, Nasim Sirjani, Ardavan Akhavan, Isaac Shiri, Hossein Arabi, Morteza Sanei Taheri, and Mohammad Kazem Tarzamni. "Fast and accurate U-net model for fetal ultrasound image segmentation." Ultrasonic Imaging 44, no. 1 (2022): 25-38.

[18] Zheng, Weimin, Linxueying Zhou, Qingwei Chai, Jianguo Xu, and Shangkun Liu. "Fully automatic analysis of muscle B-mode ultrasound images based on the deep residual shrinkage U-net." Electronics 11, no. 7 (2022): 1093.

[19] Guo, Jing-Yi, Yong-Ping Zheng, Qing-Hua Huang, and Xin Chen. "Dynamic monitoring of forearm muscles using one-dimensional sonomyography system." Journal of Rehabilitation Research & Development 45, no. 1 (2008).

[20] Azizi, Emanuel, Elizabeth L. Brainerd, and Thomas J. Roberts. "Variable gearing in pennate muscles." Proceedings of the National Academy of Sciences 105, no. 5 (2008): 1745-1750.

[21] Randhawa, Avleen, Meghan E. Jackman, and James M. Wakeling. "Muscle gearing during isotonic and isokinetic movements in the ankle plantarflexors." European journal of applied physiology 113 (2013): 437-447.

[22] Farris, Dominic James, and Glen A. Lichtwark. "UltraTrack: Software for semi-automated tracking of muscle fascicles in sequences of B-mode ultrasound images." Computer methods and programs in biomedicine 128 (2016): 111-118.

[23] Kang, Brian Byunghyun, Daekyum Kim, Hyungmin Choi, Useok Jeong, Kyu Bum Kim, Sungho Jo, and Kyu-Jin Cho. "Learning-based fingertip force estimation for soft wearable hand robot with tendon-sheath mechanism." IEEE Robotics and Automation Letters 5, no. 2 (2020): 946-953.

[24] Rho, Eojin, Daekyum Kim, Hochang Lee, and Sungho Jo. "Learning fingertip force to grasp deformable objects for soft wearable robotic glove with tsm." IEEE Robotics and Automation Letters 6, no. 4 (2021): 8126-8133.

[25] Ciritsis, Alexander, Cristina Rossi, Matthias Eberhard, Magda Marcon, Anton S. Becker, and Andreas Boss. "Automatic classification of ultrasound breast lesions using a deep convolutional neural network mimicking human decision-making." European radiology 29 (2019): 5458-5468.

[26] Hochreiter, Sepp, and Jürgen Schmidhuber. "Long short-term memory." Neural computation 9, no. 8 (1997): 1735-1780.

[27] Krizhevsky, Alex, Ilya Sutskever, and Geoffrey E. Hinton. "ImageNet classification with deep convolutional neural networks." Communications of the ACM 60, no. 6 (2017): 84-90.

[28] Gionfrida, Letizia, Wan MR Rusli, Angela E. Kedgley, and Anil A. Bharath. "A 3dcnn-lstm multi-class temporal segmentation for hand gesture recognition." Electronics 11, no. 15 (2022): 2427.

[29] Wolf, Thomas, Lysandre Debut, Victor Sanh, Julien Chaumond, Clement Delangue, Anthony Moi, Pierric Cistac et al. "Transformers: State-of-the-art natural language processing." In Proceedings of the 2020 conference on empirical methods in natural language processing: system demonstrations, pp. 38-45. 2020.

[30] He, Kaiming, Xiangyu Zhang, Shaoqing Ren, and Jian Sun. "Deep residual learning for image recognition." In Proceedings of the IEEE conference on computer vision and pattern recognition, pp. 770-778. 2016.

[31] Gionfrida, Letizia, Daekyum Kim, Davide Scaramuzza, Dario Farina, and Robert D. Howe. "Wearable robots for the real world need vision." Science Robotics 9, no. 90 (2024): eadj8812.

[32] Hafthorsdottir, Soley, Sergei Vostrikov, Andrea Cossettini, Michael Rieder, Christoph Leitner, Michele Magno, and Luca Benini. "Automatic extraction of muscle fascicle pennation angle from raw ultrasound data." In 2022 IEEE Sensors Applications Symposium (SAS), pp. 1-5. IEEE, 2022.